Published by
NIGERIAN SOCIETY OF PHYSICAL SCIENCES
Available online @ https://journal.nsps.org.ng/index.php/jnsps

J. Nig. Soc. Phys. Sci. 6 (2024) 2103

Journal of the Nigerian Society of Physical Sciences

Computational investigation and biological activity of selected Schiff bases

Segun D. Oladipo[a,*], Adesola A. Adeleke[a], Abosede A. Badeji[b], Katherine I. Babalola[a], Ayomide H. Labulo[c], Ibrahim Hassan[c], Sodiq T. Yussuf[a], Samuel O. Olalekan[d]

[a]*Department of Chemical Sciences, Olabisi Onabanjo University, Ago-Iwoye, P.M.B. 2002, Nigeria*
[b]*Department of Chemical Sciences, Tai Solarin University of Education, Ijagun, Ogun-State, Nigeria*
[c]*Department of Chemistry, Federal University of Lafia, P.M.B. 146, Lafia, Nasarawa State, Nigeria*
[d]*Department of Physiology, Olabisi Onabanjo University, Ago-Iwoye, P.M.B. 2002, Nigeria*

Abstract

This study reports the synthesis and computational investigation of two Schiff bases: (E)-N-(4-bromophenyl)-1-(2,6-dichlorophenyl)methanimine (S1) and (E)-4-(((4-bromophenyl)imino)methyl)phenol (S2), with a focus on their potential antibacterial activity. Schiff bases, known for their versatility and application in medicinal chemistry, are synthesized through the condensation reactions of the appropriate aniline with aldehydes. The molecular structures of S1 and S2 were elucidated using basic spectroscopic methods such as Fourier-transform-infrared, ultraviolet-visible as well as ^{1}H and ^{13}C-NMR, while the purity of the compounds was ascertained using elemental analysis. The stability, chemical reactivities, and electronic properties of S1 and S2 were evaluated using Density Functional Theory (DFT). The energy band gap (ΔE) of S1 and S2 is 2.81 eV and 3.02 eV, respectively, and this infers that S1 is more reactive as well as less stable than S2. The molecular electrostatic potential (MEP) mapping evaluation showed that both S1 and S2 have more of the yellow, green, and red regions than the blue region, signifying that these structures are prone to electrophilic attack. The compounds were screened against two Gram-negative (Klebsiella pneumoniae and Pseudomonas aeruginosa) and one Gram-positive bacteria (Staphylococcus aureus) to evaluate their antibacterial potential. S1 as well as S2 showed antibacterial potential against Staphylococcus aureus and exhibited less or no activity against Klebsiella pneumoniae and Pseudomonas aeruginosa. In silico studies of S1 and S2 against Staphylococcus aureus were carried out, and the outcomes corroborated the experimental findings. Pharmacological evaluation of S1 and S2 showed that both compounds exhibited less violation of Lipinski's rule of five (Ro5), which makes them less toxic and orally available.

DOI:10.46481/jnsps.2024.2103

Keywords: Schiff base, DFT, Molecular docking, Antibacterial

Article History :
Received: 26 April 2024
Received in revised form: 29 April 2024
Accepted for publication: 05 July 2024
Published: 21 July 2024

Communicated by: E. Etim

1. Introduction

Schiff bases are known to have imine (—CH=N—) as a functional group, and the nitrogen in imine could be joined to various groups such as aryl, alkyl, heterocyclic, or cycloalkyl

*Corresponding Author Tel. No.: +234-706-296-2567;
Email address: segun.oladipo@oouagoiwoye.edu.ng (Segun D. Oladipo)

but not hydrogen ($R_2C{=}NR_1$, $R_1 \neq H$) [1–3]. The condensation reaction between a carbonyl compound (aldehyde or ketone) and a primary amine in the presence of a catalyst such as, glacial acetic acid at appropriate reaction conditions affords Schiff bases [4–6]. In medicine, they have been explored as antibacterial [2], free radical scavengers [4], antidiabetics [7], anticancer [8], among others. The imine group plays a vital role in their biological and chemical activities [9]. They are also useful in polymer, corrosion and coordination chemistry [10, 11]. Due to their simple method of preparation and the ease to tune their electronic and chemical properties, Schiff bases are still relevant in modern medicine [12].

The danger posed by antimicrobial resistance to the public health sector still remains a major concern all over the world [13]. Regardless of the various means used by various antibiotics to curb bacteria, their resistance to these drugs keeps increasing [14]. Bacteria resist drugs in various ways, but it basically depends on the structure of the antibacterial agents as well as the mechanism by which they act. The ways bacteria resist drugs include altering the structure of the drug, keeping out inhibiting steps, lowering the intracellular concentration of drugs, and abnormally increasing the target enzymes by the bacteria [14, 15]. In addition to antimicrobial resistance, the emergence of new infectious diseases is on the rise. Thus, the urgent need to develop novel antimicrobial drugs with excellent activities and more importantly exhibiting unique ways of acting that differ from the ones commercially available whose well-known pathogens resist [15]. In drug discovery and development, computational techniques have been explored to investigate ligand-target interactions and binding. This gives insight on how drug molecules inhibit biomolecular targets in diseases [16]. For this study, appropriate molecular docking software was used to study the interaction of synthesized Schiff bases and protein targets of Staphylococcus aureus to complement our experimental findings. Herein, we investigate the antibacterial potential of two Schiff bases prepared from 4-bromoaniline and benzaldehyde derivatives using in vitro and in silico studies. We also use DFT to probe into the stability, chemical reactivity, and electronic properties of the synthesized compounds.

2. Experiment

2.1. Materials

Solvents used for this study are ACS reagent grades (purity ≥ 99.5 %) and were used as obtained without further purification, while 2,6-dichlorobenzaldehyde (97%), 4-hydroxybenzaldehyde (99 %) and 4-bromoaniline (97%) were purchased from Sigma Aldrich.

2.2. Instrumentation

Bruker Avance^{III} 600 MHz spectrometer was used to record the spectra for ^{1}H & ^{13}C NMR at 25 °C. $CDCl_3$ was used to prepare the solution for the NMR analysis, and the peaks at δ 7.26 and δ 77.00 ppm are the residual peaks for $CDCl_3$ in ^{1}H and ^{13}C NMR, respectively. Vario elemental EL cube CHNS analyzer was used to determine the elemental compositions of the compounds, while the electrothermal (9100) was used to measure the melting points of S1 and S2. A PerkinElmer Universal ATR spectrum 100 FT-IR spectrometer was used to record the IR spectra, while a Shimadzu UV-Vis-NIR spectrophotometer was used to obtain the electronic spectra.

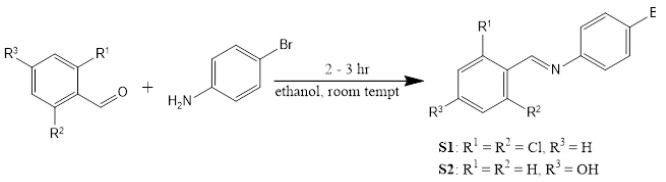

Figure 1. Schematic diagram of synthesis of compound S1 and S2.

2.3. Procedure for the preparation of S1 and S2

The procedure used previously by our group was utilized in synthesizing S1 as well as S2 with a slight modification [4, 17]. The appropriate amount of 4-bromoaniline was dissolved in ethanol and stirred for 10 min to ensure a miscible solution. Thereafter, an equimolar quantity of the aldehyde was added, and stirring continued for 2 – 3 hr (Figure 1). The off-white solids precipitated from the solution were washed three times with hexane to expunge amines that were not used up in the reaction. The purified samples were dried over the night and

2.3.1. Synthesis of (E) − N − (4 − bromophenyl) − 1 − (2, 6 − dichlorophenyl)methanimine

Compound S1 (off-white powder) was obtained by the reaction between 2,6-dichlorobenzaldehyde (0.35 g, 2 mmol) and 4-bromoaniline (0.34 g, 2 mmol) in 20 mL of absolute ethanol. Yield: 79% M.p: 178-179 °C. ^{1}H-NMR (d-chloroform, 600 MHz): δ (ppm) 7.06 (d, 2H, J_{HH} = 6, Ar-H), 7.21 (t, 1H, J_{HH} = 6, Ar-H), 7.32 (d, 2H, J_{HH} = 12, Ar-H), 7.46 (d, 2H, J_{HH} = 12, Ar-H), 8.57 (s, 1H, -CH=N). ^{13}C NMR ($CDCl_3$, 150 MHz) δ (ppm): 120.21, 122.51, 128.97, 129.75, 130.96, 132.30, 135.22 and 150.41. IR υ (cm^{-1}): 3074(w), 1631(s), 1559(s), 1429(s), 892(s), 815(m). Anal. calcd for $C_{13}H_8BrCl_2N$: C, 47.46; H, 2.45; N, 4.26; Found: C, 47.32; H, 2.29; N, 4.11.

2.3.2. Synthesis of (E)-4-(((4-bromophenyl)imino)methyl) phenol

Compound S2 (off-white powder) was obtained by the reaction between 4-hydroxybenzaldehyde (0.244 g, 2 mmol) and 4-bromoaniline (0.34 g, 2 mmol) in 20 mL of absolute ethanol. Yield: 86% M.p: 139-140 °C. ^{1}H-NMR (d-chloroform, 600 MHz): δ (ppm) 6.83 (d, 2H, J_{HH} = 6, Ar-H), 7.11 (d, 2H, J_{HH} = 6, Ar-H), 7.49 (d, 2H, J_{HH} = 12, Ar-H), 7.71 (d, 2H, J_{HH} = 12, Ar-H), 8.39 (s, 1H, -CH=N), 10.11 (s, 1H, Ar-OH). ^{13}C NMR ($CDCl_3$, 150 MHz) δ (ppm): 116.15, 118.19, 123.57, 127.79, 131.31, 132.30, 151.66, 161.20 and 161.32. IR υ (cm^{-1}): 3338(s), 2893(w), 1621(s), 1575(s), 1481(s), 1070(m), 822(m). Anal. calcd for $C_{13}H_{10}BrNO$: C, 56.55; H, 3.65; N, 5.07; Found: C, 55.42; H, 3.32; N, 4.97.

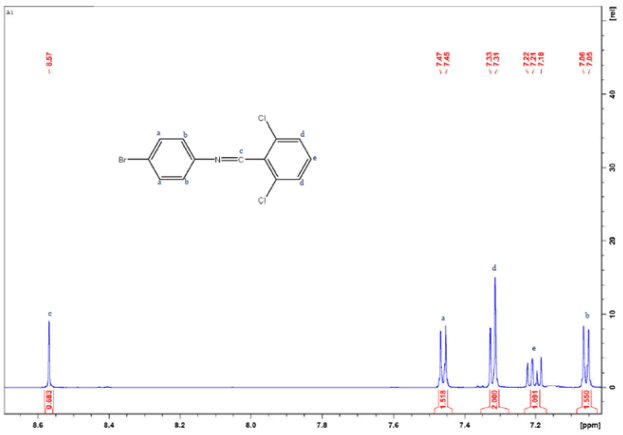

Figure 2. ^{1}H-NMR spectrum for S1.

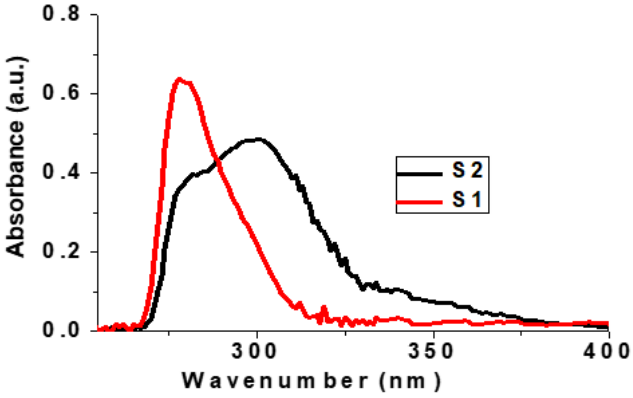

Figure 3. UV-visible spectra of S1 and S2.

2.4. Computational studies

2.4.1. Density Functional Theory (DFT)

All calculations carried out in this study were performed using the density functional theory (DFT) method, which was run using the Gaussian 16 program package [18] accessible on the Lengua cluster of the Centre for High Performance Computing [CHPC, www.chpc.ac.za], Cape Town, South Africa. The GaussView 6.0.16 graphical interface program [19] was used to create the input files, model the chemical structures for the Gaussian calculation, and visualize structures before and after calculation; thus, it was used for the 3D modeling of the substrates S1 and S2 discussed in this research work. For the geometry optimization, the M06-L [20] DFT method was employed. The basis sets used to describe the main group elements (C, H, N, O, and Cl) and the Br atom were 6-31G(d) [21] and the def2-TZVP [22] respectively.

The Molecular Electrostatic Potential (MESP) map is a powerful tool for determining a molecule's chemical reactivity, particularly in terms of electrophilic and nucleophilic attacks [23]. In this study, the MESPs of S1 and S2 were computed at the same level of theory and visualized with the GaussView 6.0.16 software. This visualization used colour grading to represent both positive and negative potential regions: the red region represents the highest negative potential, indicating a preferred site for electrophilic attack; the green region represents a neutral electrostatic area; and the blue region represents the maximum positive potential, indicating an affinity for nucleophiles.

The Frontier Molecular Orbital (FMO) analysis is a frequently used method for revealing the optical and electronic characteristics of organic molecules while also understanding their chemical reactivity [24]. The FMO parameters, including the energy levels of the Highest Occupied Molecular Orbital (HOMO) and Lowest Unoccupied Molecular Orbital (LUMO), as well as the energy gap between them (HOMO-LUMO energy gap), are crucial for determining the most reactive sites in π-electron systems [25]. The energy of the HOMO corresponds to a molecule's readiness to release electrons, indicating its ionization potential (IP). Thus, molecules with high HOMO energy tend to interact with electrophiles in certain processes. In contrast, the LUMO, being in the innermost orbital, indicates the molecule's readiness to accept electrons, and its energy is associated with electron affinity in chemical reactions [26]. Thus, molecules with low LUMO energy are vulnerable to nucleophilic attacks. The HOMO-LUMO energy gap represents the energy required to move electrons from the HOMO to the LUMO. It provides information about the molecule's charge transfer interactions. A low HOMO-LUMO energy gap suggests significant chemical reactivity but low kinetic stability [27]. In this study, FMO analysis was performed on optimized geometries in the gas phase at the same level of theory.

Moreover, quantum chemical descriptors such as global hardness (η), global softness (σ), chemical potential (μ), electronegativity (χ), and electrophilicity index (ω) can further define the chemical reactivity and stability of structures [28–31]. Global hardness [32] refers to a structure's resistance to changes in electron density, whereas chemical potential (μ) [33] provides insights on the stability, reactivity, and electronic structure of molecules. Electronegativity (χ) [30] refers to a molecule's ability to attract electrons and corresponds to a negative chemical potential (μ). The electrophilicity index [31] describes a molecule's reactivity towards electron-rich species, or nucleophiles. These descriptors collectively provide a comprehensive understanding of a molecule's behaviour and its interactions within a chemical system. Hence, they were determined using equations 1–5.

$$\eta = \frac{IP - EA}{2}, \tag{1}$$

$$\sigma = \frac{1}{\eta}, \tag{2}$$

$$\mu = \frac{E_H + E_L}{2}, \tag{3}$$

$$\chi = -\mu, \tag{4}$$

$$\omega = \frac{\mu^2}{2\eta}, \tag{5}$$

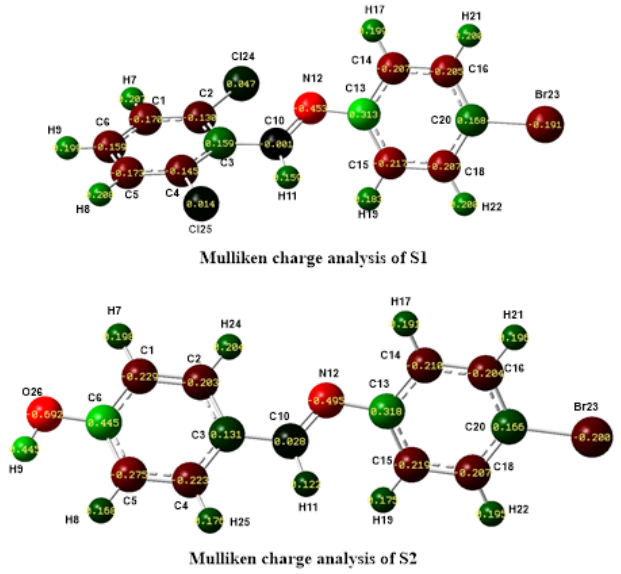

Figure 4. Mulliken charge analysis of S1 and S2 at the M06-L/6-31G(d) level of theory.

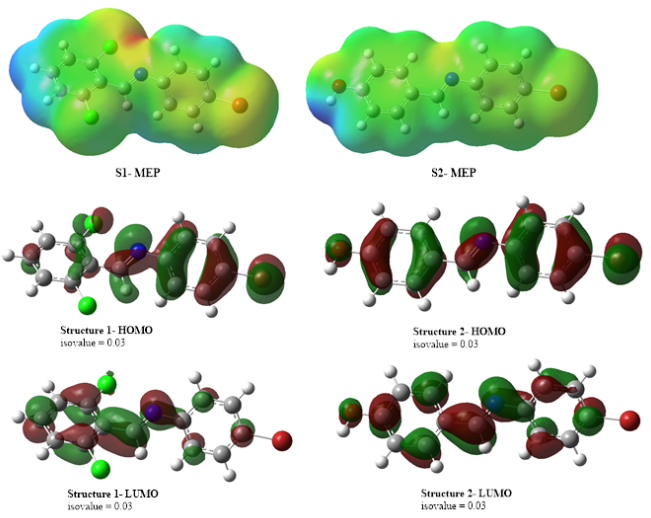

Figure 5. The molecular electrostatic potential (MESP) map and the FMO analysis of S1 and S2 computed at the M06-L/6-31G(d) level of theory.

where E_L and E_H are the energies of LUMO and HOMO, respectively, in electron volt (eV). Unless specified otherwise, all DFT computations were carried out at the M06-L/6-31G(d)[def2-TZVP] level of theory.

2.4.2. *In-silico investigation against peptidoglycan targets of Staphylococcus aureus*

The protein targets were downloaded from an online database- RCSB, in pdb format while the structure of the Schiff bases was designed with MarvinSketch and later converted to pdbqt format with OpenBabel. Penicillin, an approved drug for the treatment of microbial infections due to Staphylococcus aureus, was used as a standard, and its structure was downloaded from Pubchem and converted to pdbqt format with the same method as in the case of the Schiff bases. Autodock 4.2 was used to prepare the macromolecules, that is, the target proteins, by removing water, adding hydrogens, and computing gasteiger charges; the dimensions of the grid box for each target were also determined [34]. Docking of the pdbqt format of the ligands against each target was carried out using Autodock Vina, and the conformations with the highest binding affinity were considered for post docking analysis with Ligplot, UCSF ChimeraX [35]. The conformations were retrieved from Autodock Vina and loaded into the various softwares for the purpose of visualization. Ligplot was used to visualize the intermolecular interactions (hydrogen bonds, covalent bonds, and hydrophobic interactions), while the location of penicillin and the Schiff bases within the targets' binding pockets was visualized with UCSF ChimeraX.

2.5. *In-vitro antibacterial test*

The antibacterial potential of S1 together with S2 was investigated using two gram-negative bacteria viz: *Klebsiella pneumoniae* as well as *Pseudomonas aeruginosa* and one gram-positive viz *Staphylococcus aureus.* This was determined using the agar well diffusion method. A volume of test organism inoculum (0.5 McFaland Standard) was spread over the entire Mueller Hilton agar plate to inoculate it, and a hole of 6 mm diameter was punched into the plate in the absence of germs using a sample-filled sterile cock borer. The sterile cock borer contained the tested samples at varying concentrations in terms of percentage (100%, 50% and 38%) of 0.1 ml of each. The injected agar plates were incubated at conditions appropriate for the test organisms. Antibacterial activities in terms of the minimum inhibition concentration (MIC) and minimum bactericidal concentration (MBC) of the sample were indicated by clear zones around the punched well with DMSO as a negative control because it displayed no activity against any of the bacterial strains [36].

3. Results and Discussion

3.1. *Spectroscopic studies*

3.1.1. *^1H and ^{13}C NMR*

The ^{1}H as well as ^{13}C-NMR data of S1 and S2 were obtained in deuterated chloroform, and peaks were assigned using 2-dimensional NMR. The absence of peaks between 0 ppm and 6.83/7.06 ppm in both compounds affirmed the unavailability of aliphatic protons in their structures. Peaks due to aromatic protons in S1 and S2 were observed around 6.83 – 7.71 ppm as either singlet, doublet, triplet or quintet (Figure 2). The azomethine (imine) proton for S1 and S2 appeared at 8.57 and 8.39 ppm, respectively, and these are comparable to peaks of related compounds reported in the literature [5, 37]. In the carbon-13 NMR spectra of S1 and S2, there were no signals between 0 and 116/120 ppm, which indicates the absence of aliphatic carbons in their structures (Figures S2 & S4). The imine carbon (—CH=N) appeared around 161 ppm in the compounds.

Table 1. Quantum chemical descriptors of S1 and S2 at the M06-L/6-31G(d) level of theory.

Parameters	Δ E(eV)	E_{HOMO} (eV)	E_{LUMO} (eV)	EA (eV)	IP (eV)	η (eV)	σ (eV^{-1})	μ (D)	χ (eV)	ω (eV)
S1	2.81	-5.51	-2.70	2.70	5.51	1.41	0.71	-4.10	4.10	5.98
S2	3.02	-5.20	-2.18	2.18	5.20	1.51	0.66	-3.69	3.69	4.50

Table 2. Antibacterial potential of S1 and S2 against selected bacterial strains in mg/mL.

	MIC (mg/mL)			MBC (mg/mL)		
Compounds	K. Pneumonia	P. aeruginosa	S. aureus	K. Pneumonia	P. aeruginosa	S. aureus
S1	NA	NA	2	NA	NA	3
S2	1	NA	2	NA	NA	3

NA = No activity

3.1.2. UV-visible and FT-IR spectra

The UV-visible spectra of S1 and S2 were recorded in dichloromethane in the range of 200–400 nm (Figure 3). One major band was observed around 278 – 280 nm in the spectrum of S1 due to the π→π* transition of the imine (-C=N-) group. In the spectrum of S2, two bands (one shoulder and one broad band) were observed around 278 – 280 nm and 298 - 300 nm and these can be ascribed to the π→π* transition of the imine functional group and aromatic O−H, respectively [8, 12].

In the IR spectra of the compounds, two diagnostic peaks of sp^3 C−H and $\upsilon(-C=N)_{str}$ appeared around 3074 – 2893 cm^{-1} and 1631 – 1620 cm^{-1} respectively. A broad vibrational peak due to aromatic —OH appeared around 3337 cm^{-1} in the spectrum of S2 but was absent in S1. The vibrational band due to $\upsilon(-C=C-)_{str}$ of aromatic also appeared around 1558 – 1574 cm^{-1} in both spectra.

3.2. DFT studies

The examination of the optimized geometry of S1 reveals that the C10=N12 bond is linked to two fragments; the bromophenyl group connected to N12 and the dichlorophenyl group connected to C10. For S2, the C10=N12 is also linked to the bromophenyl group, but the second fragment is a hydroxylphenyl group, which is bonded to C10 (Figure 4). These two structures differ in the dihedral angle around the C2-C3-C10-N12. S1 has a dihedral angle of 25.6° around this angle, and S2, 1.6°at this angle. The Mulliken population method proves valuable in elucidating the reactive behavior of molecules during chemical reactions[38]. Atomic charges determined through this method are pivotal in quantum chemical examinations, influencing bond lengths, dipole moments, molecular polarizability, electronic structure, and defining molecular electrostatic potential surfaces [39]. The net atomic charge values for S1 and S2 were determined through Mulliken population analysis. All carbon atoms in S1 have negative charges except for C3, C13, and C20, which are positively charged (with C13 being the most electropositive atom). For S2, all carbons are negatively charged except for C3, C6, C10, C13, and C20, which are positively charged (C6 being the most electropositive carbon atom). The nitrogen atom (N12) and the bromine atom (Br23) in the two structures have negative charges. This analysis suggests the electropositive atoms, which are electron-deficient, are susceptible to nucleophilic attack, while the negatively charged atoms, which are electron-rich are attracted to electrophiles. Although in S1, C13 is the most positively charged atom due to its proximity to the electronegative nitrogen atom and its para orientation to the bromide ion, C6 remains the most electropositive atom in S2 and not C13 due to the former's proximity to the electron withdrawing oxygen atom (O26) of the hydroxyl group, which is more electronegative than the nitrogen atom (N12) (Figure 4). In agreement, the MESP analysis also showed that both S1 and S2 have more of the yellow, green and red regions than the blue region, signifying that these structures are prone to electrophilic attack. The FMO analysis showed that for S1, the HOMO is mainly located on the bromophenyl fragment rather than on the dichlorophenyl fragment, while the LUMO is located more on the dichlorophenyl fragment than on the bromophenyl fragment. For S2, the fragment orbitals are highly filled HOMO, while examination of the LUMO suggests the orbitals are partially filled (Figure 5). With the negative HOMO energy values of -5.51 eV and -5.20 eV for S1 and S2 respectively, and the negative LUMO energy values of -2.70 eV and -2.18 eV respectively, S1 and S2 are believed to be stable compounds. Koopman's theorem [40] establishes a relationship between the energy values of the HOMO and the LUMO with the ionization potential (IP = $-E_{HOMO}$) and electron affinities (EA = $-E_{LUMO}$), respectively. The ionization potential (IP) and electron affinities (EA) are determined as the negative energy eigenvalues of the HOMO and LUMO, respectively. Again, studies have shown that compounds with a small ΔE ($E_{HOMO-LUMO}$ energy gap) are highly reactive and less stable [41]. The ΔE for both S1 (2.81 eV) and S2 (3.02 eV) implies that they are very reactive; however, S1 is computed to be more reactive and less stable than S2.

Moreover, compounds with low chemical reactivity and high stability are considered to be hard, while those with high chemical reactivity and low stability are considered soft. Also, a compound is said to be very reactive if it possesses a low global hardness value and a high global softness value. For both structures, the η values are 1.41 eV and 1.51 eV for S1 and S2 respectively, and the σ are 0.71 eV and 0.66 eV for S1 and S2 respectively. Although the low η in both structures indicates high reactivity, S1 is computed to be more reactive than S2 from a global softness standpoint. The global electrophilicity index

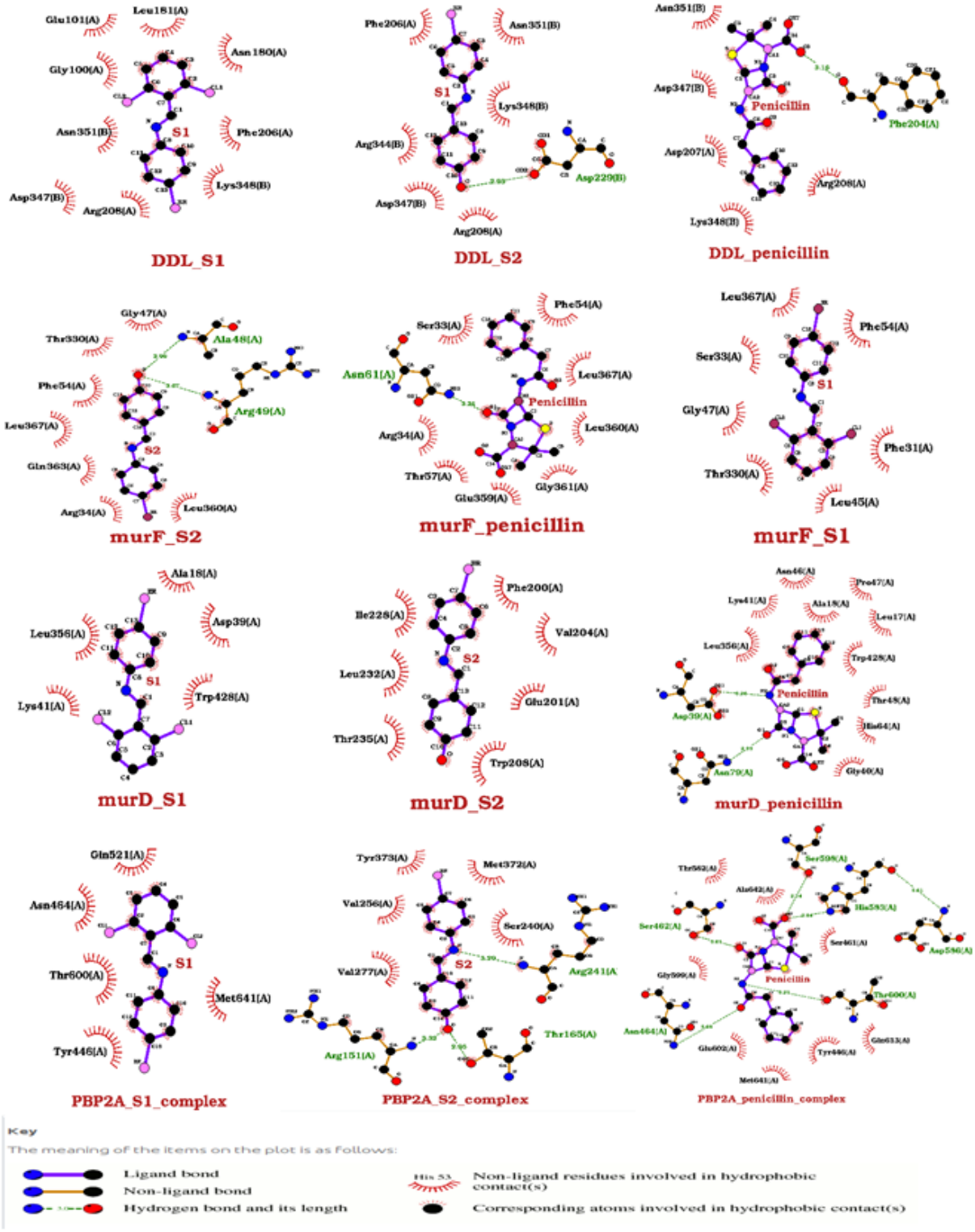

Figure 6. Ligplot snapshots showing the Ligands interaction with the protein residues.

ω shows the electrophilic power of molecules and electronegativity (χ) denotes the molecule's electron-donating characteristics. Compounds with high χ and ω values signify that they are highly electrophilic, and such would attract nucleophiles. From Table 1, the χ values for S1 and S2 are 4.10 and 3.69 respectively, and the ω values for S1 and S2 are 5.98 and 4.50, respectively. With the higher values of χ and ω for S1 than S2, S1 is also described to be more electrophilic than S2, and also accepts electrons more from an interacting molecule than S2.

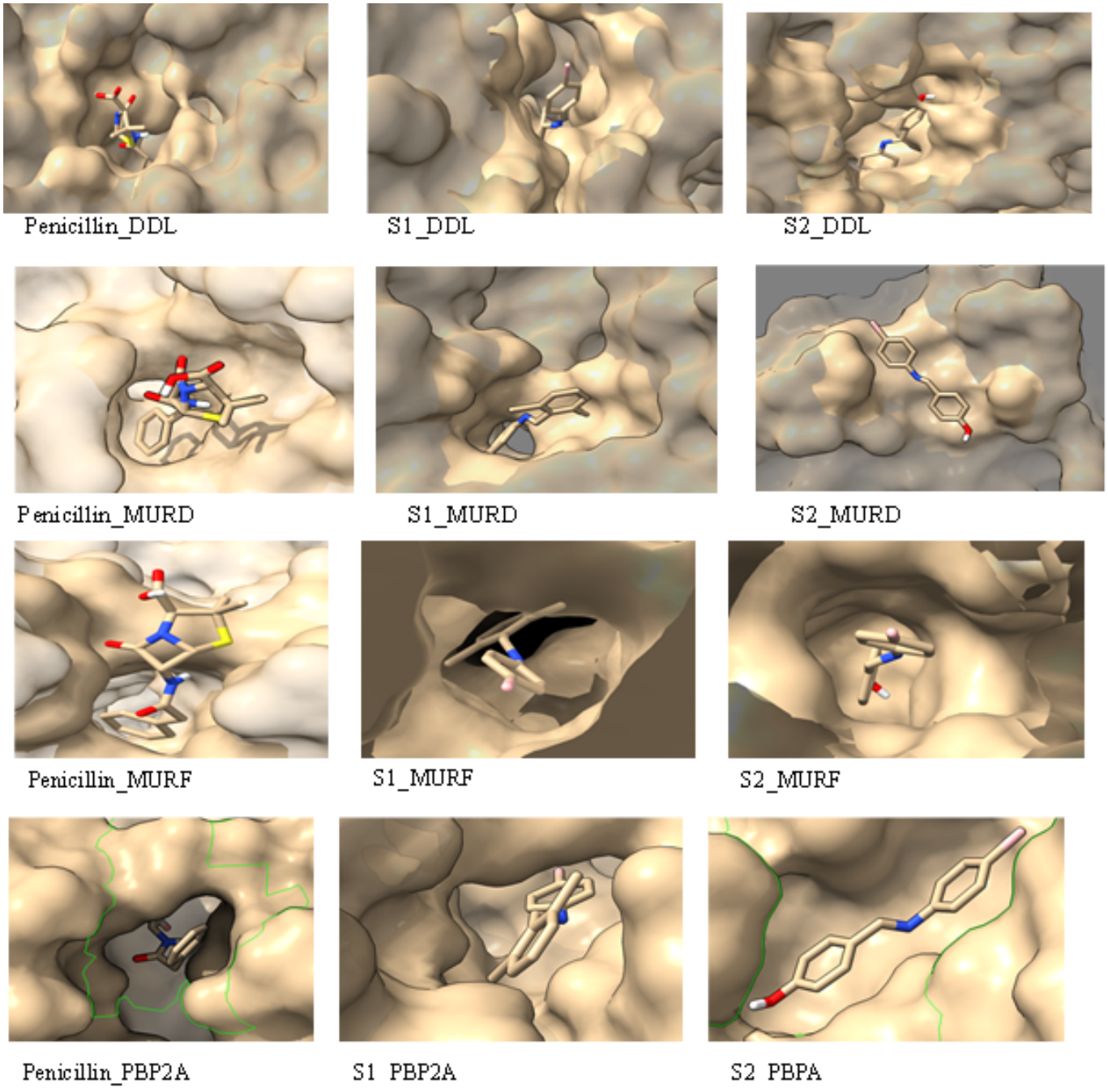

Figure 7. Snapshots showing the location of the ligands within the protein's binding pockets.

3.3. *In-vitro antibacterial activity*

The antibacterial screening of S1 and S2 was against two Gram-negative (P. aeruginosa, and K. pneumonia) and one Gram-positive bacteria (*S. aureus*). The antibacterial potential of S1 and S2 was measured using minimum inhibitory concentrations (MIC) and minimum bactericidal concentrations (MBC). MIC literally means the lowest concentration at which a drug will inhibit the visible growth of a microorganism, while MBC means the lowest concentration of an antimicrobial agent that will effectively prevent the growth of a microorganism. Lower MIC and MBC values indicate higher antibacterial potential. S1 and S2 exhibited no antibacterial activity against P. aeruginosa Table 2. This could be attributed to the inability of S1 and S2 to penetrate through the bacteria strain or perhaps being modified or degraded as they enter the cell wall of P. aeruginosa [42]. Against K. pneumonia,S2 displayed moderate activity based on the MIC value but showed no activity based on the MBC value. However, our findings showed that S1 has no antibacterial potential against *K. pneumonia*. Interestingly, both compounds exhibited moderate activity against S. aureus,

as seen in Table 2.

3.4. In silico studies

Following the results from the in vitro antibacterial studies of both compounds against three bacteria strains, namely Klebsiella sp., Pseudomonas sp., and Staphylococcus aureus, it was observed that the minimum bactericidal and inhibitory concentrations of both compounds against Staphylococcus aureus were quite remarkable and similar. For this reason, a molecular docking study was carried out to gain insight into the interaction of the synthesized compounds and targets of S. aureus. Reports had shown that, promising drug candidates used for combating S. aureus target the cell wall as well as the cell membrane and, in some cases, alter the RNA/DNA, protein, and folic acid synthesis [43]. The cell wall of S. aureus was once a good target for antibiotics; however, due to the adaptation of the proteins of the cell wall, i.e., penicillin-binding proteins 2A (PBP2A), to common antibiotics, other mechanisms, such as targeting the proteins responsible for the synthesis of the cell wall, have been explored [44]. These proteins responsible for the synthesis of the cell wall include UDP-N-acetylmuramoyl-L-alanyl-D-glutamatesynthetase (MURD), UDP-N-acetylmuramoylalanyl-D-D-glutamyl-2,6-diaminopimelate-D-alanyl-D-alanyl ligase (MURF) and protein-D-alanyl-alaninesynthetaseA (DDL) [45]. For this study, we targeted MURD, MURF, DDL and PBP2A of S. aureus with S1 and S2 to understand the interaction between the synthesized compounds and S. aureus. Any compounds that could inhibit these proteins would disrupt the steps leading to the synthesis of the cell wall, thus resulting in the death of the cells. Table 3 shows the free energy values of the docking processes of the ligands with the macro molecules. It is evident that S1 and S2 have some levels of interactions with all the macro molecules, although at different levels, which is majorly due to the type of interactions as shown in Figure 6. According to the binding interactions in the Ligplot and UCSF ChimeraX snapshots in Figures 6 and 7), the hydrogen bond interactions between amino acid residues of PBP2A and oxygen from ketone, as well as the nitrogen from the amide group in penicillin, seem to aid its higher binding energy and deeper position within the binding cavity of the target. Three hydrogen bonds due to the -OH and -C=N groups are also visible in S2, which seem to boost its binding energy and deepen its position within the binding pocket than S1 which has pure hydrophobic interactions and is only slightly buried.

In MURF, penicillin forms just one hydrogen bond and is bound at the surface and not within a binding pocket; its binding energy is also lower compared to S2, which forms two hydrogen bonds with the target's residues. In PBP2A, the docking scores of penicillin, outshined the one for S1 and S2. Penicillin has the highest binding energy with MURD and is buried deep, unlike S1 and S2, with only hydrophobic interactions and at surficial positions. There is not much difference between the binding energies of the ligands with DDL, as S2 and Penicillin each have just one hydrogen bond with the target, although S2 is deeply buried within the pocket. S1, as is the case with other targets, forms only hydrophobic interactions and is slightly buried.

Table 3. Free energy values of the ligands against cell wall macromolecules of Staphylococcus aureus.

Macromolecules	Ligands	Free energy value (kJ/mol)
MURD	Penicillin	-6.9
	S1	-6.3
	S2	-5.1
MURF	Penicillin	-8.0
	S1	-8.6
	S2	-8.2
PBP2A	Penicillin	-7.6
	S1	-6.7
	S2	-6.9
DDL	Penicillin	-6.8
	S1	-7.0
	S2	-6.9

The interaction of S1 with the proteins seems to improve with hydrophobicity, as is evident from its higher free energy values when compared to the ones for S2 in most complexes. In Figure 7, it can be seen that S1 is more buried than S2. Also, S2 has covalent interactions with MURF and DDL, and this seems to be an advantage because it is deeply buried in the cavities of this macromolecule when compared to MURD and PBP2A, where its interaction is surficial. S1 and S2 displayed higher docking scores with DDL and MURF relative to the reference drug (penicillin) used in this study. For example, the docking scores for S1 and S2 with MURF are -8.6 and -8.2 $kJmol^{-1}$, while the one for penicillin is -8.0 $kJmol^{-1}$. However, for PBP2A (the target for penicillin) and MURD, penicillin outshined both S1 and S2 i.e., the docking scores for penicillin against PBP2A were -7.6 kJ/mol, while for S1 and S2, were -6.9 and 6.7 $kJmol^{-1}$, respectively. We could conclude that the molecular docking studies of S1 and S2 with cell wall macromolecules of S. aureus corroborate the experimental findings and that more work needs to be done to optimize S1 and S2 in a bid to improve their binding interactions with microbial targets, resulting in enhanced.

3.5. Drug-likeness and pharmacokinetic properties

The physicochemical and pharmacokinetic properties of S1 and S2, which in turn predict the drug-likeness of the compounds, were carried out using web-based analytical tools; SwissADME. This was achieved by uploading the 3D structures of the compounds to the SwissADME software interface, where canonical smiles were generated. Calculations were done on the generated canonical smiles to predict these parameters [46]. The results are compared with Lipinski's rule of five (Ro5) to predict the bioavailability of both compounds. Molecular weight (M.W.), hydrogen bond acceptor (H.B.A.) and donor (HBD) ability, aqueous solubility (Log S), lipophilicity (Log P), topological polar surface area (TPSA), skin permeation (LogKp), as well as rotatable bonds (RotB), were evaluated. We also predicted their pharmacokinetic parameters, such

Table 4. Free energy values of the ligands against cell wall macromolecules of Staphylococcus aureus.

	S1	S2	Acceptable threshold (Ro5)
Physicochemical properties			
Molecular weight (Da)	329.02	276.13	<500Da
LogP	4.91	3.38	<5
LogS (mol/L)	-5.53	-3.97	0 → -6
TPSA (A^2)	12.36	32.59	≤140
HBA	1	2	≤10
HBD	0	1	≤5
Rotatable bonds	2	2	<10
Pharmacokinetics properties			
GI absorption	High	High	
BBB Permeant	No	Yes	
Pg-Substrate	No	No	

as blood-brain barrier (B.B.B.) permeant, gastrointestinal (G.I.) absorption, and P-glycoprotein (P-gp) substrate [37]. The M.W. of S1 and S2 are 329.02 and 276.13 $gmol^{-1}$, respectively, and this complies with Lipinski's Ro5, indicating the bioavailability of both compounds. Also, the predicted values for H.B.D., H.B.A., and RotBs are within the range of the acceptable values of Lipinski's standard Ro5, as seen in Table 4. The predictable TPSA values for S1 and S2 fell within the standard range of ≤140Å^2 and thus easily permeate through the cells, most especially after further optimization. The acceptable values for LogS and LogP are ≤-6 and <5, respectively, and the LogP and LogS values for both compounds fell within the range. This indicates that S1 and S2 can easily permeate through the intestinal epithelium surface, which further ascertained their promising bioavailability. S1 and S2 are predicted to have high gastrointestinal absorption, and this signifies that they can easily be absorbed in the intestine, which poses both compounds as good drug candidates[16]. S2 is predicted to penetrate through the blood-brain barrier, while S1 could not. Generally, a promising drug candidate does not bind to P-gp substrates, and interestingly, S1 and S2 are not P-gp substrates.

4. Conclusion

Schiff bases S1 and S2 were successfully prepared and elucidated using different spectroscopic methods. Calculated quantum chemical descriptors such as energy band gap, HOMO, and LUMO among others, revealed that S1 is more reactive and less stable than S2. The molecular electrostatic potential (MEP) mapping analysis showed that both S1 and S2 are prone to electrophilic attack. The MICs and MBCs values revealed that both compounds exhibited antibacterial potential against *S. aureus* but showed less or no activity against *K. pneumoniae* and *P. aeruginosa*. Interestingly, both compounds deviated minimally from Lipinski's Ro5, suggesting they are orally less toxic and are bioavailable templates for the development of antibiotics in the future.

References

[1] S. A. Olagboye, T. L. Yusuf, S. D. Oladipo & S. J. Zamisa, "Crystal structure of (E)-1-(2-nitrophenyl)-N-(o-tolyl) methanimine, $C_{14}H_{12}N_2O_2$", Zeitschrift für Kristallographie-New Crystal Structures **235** (2006) 833. https://doi.org/10.1515/ncrs-2020-0034.

[2] T. L. Yusuf, S. D. Oladipo, S. A. Olagboye, S. J. Zamisa & G. F. Tolufashe, "Solvent-free synthesis of nitrobenzyl Schiff bases: Characterization, antibacterial studies, density functional theory and molecular docking studies", Journal of Molecular Structure **1222** (2020) 128857. https://doi.org/10.1016/j.molstruc.2020.128857.

[3] S. Gul, A. Alam, M. Assad, A. A. Elhenawy, M. S. Islam, S. A. A. Shah, Z. Parveen, T. A. Shah & M. Ahmad, "Exploring the synthesis, molecular structure and biological activities of novel Bis-Schiff base derivatives: A combined theoretical and experimental approach", Journal of Molecular Structure **1306** (2024) 137828. https://doi.org/10.1016/j.molstruc.2024.137828.

[4] S. D. Oladipo, R. C. Luckay, K. A. Olofinsan, V. A. Obakachi, S. J. Zamisa, A. A. Adeleke, A. A. Badeji, S. A. Ogundare, & B. P. George, "Antidiabetes and antioxidant potential of Schiff bases derived from 2-naphthaldehye and substituted aromatic amines: Synthesis, crystal structure, Hirshfeld surface analysis, computational, and invitro studies", Heliyon **10** (2024) e23174. https://doi.org/10.1016/j.heliyon.2023.e23174.

[5] S. D. Oladipo, T. L. Yusuf, S. J. Zamisa, M. Shapi & T. J. Ajayi, "Synthesis, crystal structure, Hirshfeld surface analysis and DFT studies of N-(2, 6-diisopropylphenyl)-1-(4-methoxyphenyl) methanimine", Journal of Molecular Structure **1241** (2021) 130620. https://doi.org/10.1016/j.molstruc.2021.130620.

[6] G. Venkatesh, P. Vennila, S. Kaya, S. B. Ahmed, P. Sumathi, V. Siva, P. Rajendran & C. Kamal, "Synthesis and Spectroscopic Characterization of Schiff Base Metal Complexes, Biological Activity, and Molecular Docking Studies", ACS omega **9** (2024) 8123. https://doi.org/10.1021/acsomega.3c08526.

[7] B. Adalat, F. Rahim, M. Taha, S. Hayat, N. Iqbal, Z. Ali, A. A. Shah, A. Wadood, A. U. Rehman & K. M. Khan, "Synthesis of Benzofuran–based Schiff bases as anti-diabetic compounds and their molecular docking studies", Journal of Molecular Structure **1265** (2022) 133287. https://doi.org/10.1016/j.molstruc.2022.133287.

[8] A. A. Adeleke, S. D. Oladipo, S. J. Zamisa, I. A. Sanusi & B. Omondi, "DNA/BSA binding studies and in vitro anticancer and antibacterial studies of isoelectronic Cu (I)-and Ag (I)-pyridinyl Schiff base complexes incorporating triphenylphosphine as co-ligands", Inorganica Chimica Acta **558** (2023) 121760. https://doi.org/10.1016/j.ica.2023.121760.

[9] J. Ceramella, D. Iacopetta, A. Catalano, F. Cirillo, R. Lappano & M. S. Sinicropi, "A review on the antimicrobial activity of Schiff bases: Data collection and recent studies, Antibiotics **11** (2022) 191. https://doi.org/10.3390/antibiotics11020191.

[10] M. Mishra, K. Tiwari, A. K. Singh & V. P. Singh, "Versatile coordination behaviour of a multi-dentate Schiff base with manganese (II), copper (II) and zinc (II) ions and their corrosion inhibition study, Inorganica Chimica Acta **425** (2015) 36. https://doi.org/10.1016/j.ica.2014.10.026.

[11] A. A. Adeleke, M. S. Islam, O. Sanni, C. Mocktar, S. J. Zamisa & B. Omondi, "Aryl variation and anion effect on CT-DNA binding and in vitro biological studies of pyridinyl Ag (I) complexes", Journal of Inorganic Biochemistry **214** (2021) 111266. https://doi.org/10.1016/j.jinorgbio.2020.111266.

[12] T. L. Yusuf, S. D. Oladipo, S. Zamisa, H. M. Kumalo, I. A. Lawal, M. M. Lawal & N. Mabuba, "Design of new Schiff-Base Copper (II) complexes: Synthesis, crystal structures, DFT study, and binding potency toward cytochrome P450 3A4", ACS omega **6** (2021) 13704. https://doi.org/10.1021/acsomega.1c00906.

[13] S. D. Oladipo, B. Omondi & C. Mocktar, "Synthesis and structural studies of nickel(II)-and copper(II)-N, N$\prime$-diarylformamidine dithiocarbamate complexes as antimicrobial and antioxidant agents", Polyhedron **170** (2019) 712. https://doi.org/10.1016/j.poly.2019.06.038.

[14] S. D. Oladipo, B. Omondi, & C. Mocktar "Co(III) N, N$\prime$-diarylformamidine dithiocarbamate complexes: Synthesis, characterization, crystal structures and biological studies", Applied organometallic chemistry **34** (2020) e5610. https://doi.org/10.1002/aoc.5610.

[15] E. Yousif, A. Majeed, K. Al-Sammarrae, N. Salih, J. Salimon, & B. Abdullah, "Metal complexes of Schiff base: preparation, characteriza-

tion and antibacterial activity", Arabian Journal of Chemistry **10** (2017) S1639. https://doi.org/10.1016/j.arabjc.2013.06.006.

[16] S. D. Oladipo, O.I. Akinpelu, & B. Omondi, "Ligand-Guided Investigation of a series of Formamidine Based Thiuram Disulfides as potential Dual-Inhibitors of Cox-1 and Cox-2", Chemistry & Biodiversity **20** (2023) e202200875. https://doi.org/10.1002/cbdv.202200875.

[17] S. D. Oladipo, G. F. Tolufashe, C. Mocktar & B. Omondi, "Ag (I) symmetrical N, N$\prime$-diarylformamidine dithiocarbamate PPh_3 complexes: Synthesis, structural characterization, quantum chemical calculations and in vitro biological studies", Inorganica Chimica Acta **520** (2021) 120316. https://doi.org/10.1016/j.ica.2021.120316.

[18] M. J. Frisch, G. W. Trucks, H. B. Schlegel, G. E. Scuseria, M. A. Robb, J. R. Cheeseman, G. S. Scalmani, V. P. G. A. Barone, G. A. Petersson, H. J. R. A. Nakatsuji & D. J. Fox, itGaussian 16 rev. c. 01, Wallingford CT 34 (2016). http://www.gaussian.com620(2009).

[19] R. D. I. I. Dennington, T. A. Keith & J. M. Millam, GaussView, version 6.0. 16. *Semichem Inc Shawnee Mission KS*. (2016)

[20] Y. Zhao & D. G. Truhlar, "The M06 suite of density functionals for main group thermochemistry, thermochemical kinetics, noncovalent interactions, excited states, and transition elements: Two new functionals and systematic testing of four M06-class functionals and 12 other functionals", Theor. Chem. Acc. **120** (2008) 215. https://doi.org/10.1007/s00214-007-0310-x.

[21] V. A. Rassolov, M. A. Ratner, J. A. Pople, P. C. Redfern & L. A. Curtiss, "6-31G* basis set for third-row atoms", Journal of Computational Chemistry **22** (2001) 976. https://doi.org/10.1002/jcc.1058.

[22] F. Weigend, "Accurate Coulomb-fitting basis sets for H to Rn", Physical chemistry chemical physics **8** (2006) 1057. https://doi.org/10.1039/B515623H.

[23] L. Liu, L. Miao, L. Li, F. Li, Y. Lu, Z. Shang & J. Chen, "Molecular electrostatic potential: a new tool to predict the lithiation process of organic battery materials", The Journal of Physical Chemistry Letters **9** (2018) 3573. https://doi.org/10.1021/acs.jpclett.8b01123.

[24] T. Chaudhary, M. K. Chaudhary, S. Jain, P. Tandon & B. D. Joshi, "The experimental and theoretical spectroscopic elucidation of molecular structure, electronic properties, thermal analysis, biological evaluation, and molecular docking studies of isococculidine", Journal of Molecular Liquids **391** (2023) 123212. https://doi.org/10.1016/j.molliq.2023.123212.

[25] K. Fukui, T. Yonezawa & H. Shingu, "A molecular orbital theory of reactivity in aromatic hydrocarbons", The Journal of Chemical Physics **20** (1952) 722. https://doi.org/10.1063/1.1700523.

[26] E. D. Akpan, S. D. Oladipo, T. W. Quadri, L. O. Olasunkanmi, E. E. Nwanna, B. Omondi & E. E. Ebenso, "Formamidine-based thiuram disulfides as efficient inhibitors of acid corrosion of mild steel: electrochemical, surface, and density functional theory/monte carlo simulation studies", ACS omega **7** (2022) 26076. https://doi.org/10.1021/acsomega.2c00985.

[27] A. Asghar, M. M. Bello, A. A. A. Raman, W. M. A. W. Daud, A. Ramalingam & S. B. M. Zain, "Predicting the degradation potential of Acid blue 113 by different oxidants using quantum chemical analysis", Heliyon **5** (2019) e02396. https://doi.org/10.1016/j.heliyon.2019.e02396.

[28] N. Islam & D. C. Ghosh, "The electronegativity and the global hardness are periodic properties of atoms", Journal of Quantum Information Science **1** (2011) 135. http://dx.doi.org/10.4236/jqis.2011.13019.

[29] M. Bhatia, "An overview of conceptual-DFT based insights into global chemical reactivity of volatile sulfur compounds (VSCs)", Computational Toxicology **29** (2023) 100295. https://doi.org/10.1016/j.comtox.2023.100295.

[30] W. Yang & R. G. Parr, "Hardness, softness, and the fukui function in the electronic theory of metals and catalysis", Proceedings of the National Academy of Sciences **82** (1985) 6723. https://doi.org/10.1073/pnas.82.20.6723.

[31] R. G. Parr, L. V. Szentpály & S. Liu, "Electrophilicity index", Journal of the American Chemical Society **121** (1999) 1922. https://doi.org/10.1021/ja983494x.

[32] S. D. Oladipo, S. J. Zamisa, A. A. Badeji, M. A. Ejalonibu, A. A. Adeleke, I. A. Lawal, A. Henni, & M. M. Lawal, "Ni2+ and Cu2+ complexes of N-(2, 6-dichlorophenyl)-N-mesityl formamidine dithiocarbamate structural and functional properties as CYP3A4 potential substrates", Scientific Reports **13** (2023) 13414. https://doi.org/10.1038/s41598-023-39502-x.

[33] A. A. Adeleke, S. D. Oladipo, R. C. Luckay, E. O. Akintemi, K. A. Olofinsan, I. Babatunde Onajobi, S. T. Yussuf, S. A. Ogundare, O. M. Adeleke, & K. I. Babalola, "Synthesis and Therapeutic Potential of selected Schiff Bases: In vitro Antibacterial, Antioxidant, Antidiabetic, and Computational Studies", ChemistrySelect **9** (2024) e202304967. https://doi.org/10.1002/slct.202304967.

[34] O. Trott & A. J. Olson, "AutoDock Vina: improving the speed and accuracy of docking with a new scoring function, efficient optimization, and multithreading", Journal of computational chemistry **31** (2010) 455. https://doi.org/10.1002/jcc.21334.

[35] J. Eberhardt, D. Santos-Martins, A. F. Tillack & S. Forli, "AutoDock Vina 1.2. 0: New docking methods, expanded force field, and python bindings", Journal of chemical information and modeling **61** (2021) 3891. https://doi.org/10.1021/acs.jcim.1c00203.

[36] R. M. Humphries, J. Ambler, S. L. Mitchell, M. Castanheira, T. Dingle, J. A. Hindler, L. Koeth, & K. Sei, "CLSI methods development and standardization working group best practices for evaluation of antimicrobial susceptibility tests" Journal of clinical microbiology **56** (2018) 10. https://doi.org/10.1128/jcm.01934-17.

[37] S. D. Oladipo, T. L. Yusuf, S. J. Zamisa, G. F. Tolufashe, K. A. Olofinsan, Z. Tywabi-Ngeva & N. Mabuba, "Synthesis, crystal structure with free radical scavenging activity and theoretical studies of Schiff bases derived from 1-naphthylamine, 2, 6-diisopropylaniline, and substituted benzaldehyde", European Journal of Chemistry **12** (2021) 204. https://doi.org/10.5155/eurjchem.12.2.204-215.2088.

[38] Z. Demircioğlu, C. Albayrak & O. Büyükgüngör, "Theoretical and experimental investigation of (E)-2-([3, 4-dimethylphenyl) imino] methyl)-3-methoxyphenol: Enol–keto tautomerism, spectroscopic properties, NLO, NBO and NPA analysis", Journal of Molecular Structure **1065** (2014) 210. https://doi.org/10.1016/j.molstruc.2014.02.062.

[39] P. Govindasamy, S. Gunasekaran & S. Srinivasan, "Molecular geometry, conformational, vibrational spectroscopic, molecular orbital and Mulliken charge analysis of 2-acetoxybenzoic acid", Spectrochimica Acta Part A: Molecular and Biomolecular Spectroscopy **130** (2014) 329. https://doi.org/10.1016/j.saa.2014.03.056.

[40] A. H. Pandith & N. Islam, "Comparative assessment of QSTR models based on density functional, hartree–fock, AM1, and PM3 methods for acute toxicity of aliphatic compounds toward Vibrio fischeri", International Journal of Quantum Chemistry **113** (2013) 830. https://doi.org/10.1002/qua.24133.

[41] J. I. Aihara, "Reduced HOMO− LUMO gap as an index of kinetic stability for polycyclic aromatic hydrocarbons", The Journal of Physical Chemistry A **103** (1999) 7487. https://doi.org/10.1021/jp990092i.

[42] S. D. Oladipo, C. Mocktar & B. Omondi, "In vitro biological studies of heteroleptic Ag (I) and Cu (I) unsymmetrical N, N$\prime$-diarylformamidine dithiocarbamate phosphine complexes; the effect of the metal center", Arabian Journal of Chemistry **13** (2020) 6379. https://doi.org/10.1016/j.arabjc.2020.05.039.

[43] H. Lade & J. S. Kim, "Bacterial targets of antibiotics in methicillin-resistant Staphylococcus aureus", Antibiotics **10** (2021) 398. https://doi.org/10.3390/antibiotics10040398.

[44] S. A. Khedkar, A. K. Malde & E. C. Coutinho, "Design of inhibitors of the MurF enzyme of Streptococcus pneumoniae using docking, 3D-QSAR, and de novo design", Journal of chemical information and modeling **47** (2007) 1839. https://doi.org/10.1021/ci600568u.

[45] M. Hossain, J. Farhana, M. T. Akbar, A. Chakraborty, S. Islam & A. Mannan, "Identification of potential targets in Staphylococcus aureus N315 using computer aided protein data analysis", Bioinformation **9** (2013) 187. https://doi.org/10.6026%2F97320630009187.

[46] A. Daina, O. Michielin, & V. Zoete, "SwissADME: a free web tool to evaluate pharmacokinetics, drug-likeness and medicinal chemistry friendliness of small molecules", Scientific reports **7** (2017) 42717. https://doi.org/10.1038/srep42717.